AGU PUBLICATIONS

Paleoceanography and Paleoclimatology

RESEARCH ARTICLE
10.1002/2017PA003181

Key Points:
- Southeast Indian Ocean surface hydrological conditions are impacted by Indonesian throughflow
- Pacific decadal climate variability modulated the Indonesian throughflow leakage into the Indian Ocean over the past 200 years
- Indonesian throughflow increase/decrease predominantly coincides with slowdown/acceleration of global warming, respectively

Supporting Information:
- Supporting Infomation S1

Correspondence to:
R. Hennekam,
rickhennekam@gmail.com

Citation:
Hennekam, R., Zinke, J., van Sebille, E., ten Have, M., Brummer, G.-J. A., & Reichart, G.-J. (2018). Cocos (Keeling) corals reveal 200 years of multidecadal modulation of southeast Indian Ocean hydrology by Indonesian throughflow. *Paleoceanography and Paleoclimatology*, *33*, 48–60. https://doi.org/10.1002/2017PA003181

Received 8 JUN 2017
Accepted 13 DEC 2017
Published online 4 JAN 2018

Cocos (Keeling) Corals Reveal 200 Years of Multidecadal Modulation of Southeast Indian Ocean Hydrology by Indonesian Throughflow

Rick Hennekam[1], Jens Zinke[2,3,4,5], Erik van Sebille[6,7], Malou ten Have[1,8], Geert-Jan A. Brummer[1,9], and Gert-Jan Reichart[1,8]

[1]NIOZ Royal Netherlands Institute for Sea Research, Department of Ocean Systems, and Utrecht University, Texel, Netherlands, [2]Paleontology Section, Freie Universität Berlin, Berlin, Germany, [3]Department of Environment and Agriculture, Curtin University of Technology, Bentley, WA, Australia, [4]Australian Institute of Marine Science, Nedlands, WA, Australia, [5]School of Geography, Archeology and Environmental Studies, University of Witwatersrand, Johannesburg, South Africa, [6]Grantham Institute and Department of Physics, Imperial College London, London, UK, [7]Institute for Marine and Atmospheric research Utrecht, Utrecht University, Utrecht, Netherlands, [8]Department of Earth Sciences, Faculty of Geosciences, Utrecht University, Utrecht, Netherlands, [9]Earth and Climate Cluster, Department of Earth Sciences, Faculty of Earth and Life Sciences, VU University Amsterdam, Amsterdam, Netherlands

Abstract The only low latitude pathway of heat and salt from the Pacific Ocean to the Indian Ocean, known as Indonesian Throughflow (ITF), has been suggested to modulate Global Mean Surface Temperature (GMST) warming through redistribution of surface Pacific Ocean heat. ITF observations are only available since ~1990s, and thus, its multidecadal variability on longer time scales has remained elusive. Here we present a 200 year bimonthly record of geochemical parameters (δ^{18}O-Sr/Ca) measured on Cocos (Keeling) corals tracking sea surface temperature (SST; Sr/Ca) and sea surface salinity (SSS; seawater-$\delta^{18}O$=$\delta^{18}O_{sw}$) in the southeastern tropical Indian Ocean (SETIO). Our results show that SETIO SSS and $\delta^{18}O_{sw}$ were impacted by ITF transport over the past 60 years, and therefore, reconstructions of Cocos $\delta^{18}O_{sw}$ hold information on past ITF variability on longer time spans. Over the past 200 years ITF leakage into SETIO is dominated by the interannual climate modes of the Pacific Ocean (El Niño—Southern Oscillation) and Indian Ocean (Indian Ocean Dipole). Pacific decadal climate variability (represented by the Pacific Decadal Oscillation) significantly impacted ITF strength over the past 200 years determining the spatiotemporal SST and SSS advection into the Indian Ocean on multidecadal time scales. A comparison of our SETIO $\delta^{18}O_{sw}$ record to GMST shows that ITF transport varied in synchrony with global warming rate, being predominantly high/low during GMST warming slowdown/acceleration, respectively. This hints toward an important role for the ITF in global warming rate modulation.

1. Introduction

The interocean exchange between the Pacific and Indian Oceans via the Indonesian Seas, i.e. the Indonesian Throughflow (ITF), affects the oceanic distribution of heat and salt, forming a critical choke point of the global thermohaline circulation (Durgadoo et al., 2017; Gordon, 1986; Le Bars et al., 2013; Speich et al., 2007). The ITF has been linked to the recent slowdown of global mean surface temperature (GMST) warming (~1998–2013) by promoting heat removal from the surface Pacific Ocean (Lee et al., 2015). As such, the ITF is potentially an important component affecting global climate change, and understanding its multidecadal behavior during the last two centuries is thus essential. However, instrumental observations of the ITF are currently limited to the last three decades (Gordon et al., 1999; Liu et al., 2015; Meyers, 1996), being hindcasted to the 1960s by reanalysis and model approaches (Tillinger & Gordon, 2009; van Sebille et al., 2014). To further our understanding of the multidecadal variability of the ITF and its relation with GMST, we investigate ITF transport into the southeast tropical Indian Ocean (SETIO) over the last two centuries using coral-derived sea surface temperature (SST) and salinity (SSS) proxy data from the Cocos (Keeling) atoll.

The SSS in the SETIO area and hence at the Cocos (Keeling) atoll (from here on Cocos) is strongly linked to ITF variability (Hua et al., 2004, 2005). Warm, low saline upper-ocean water is transported via the ITF into the area between Indonesia and Australia (Indo-Australian Basin; see Figure 1a), forming an

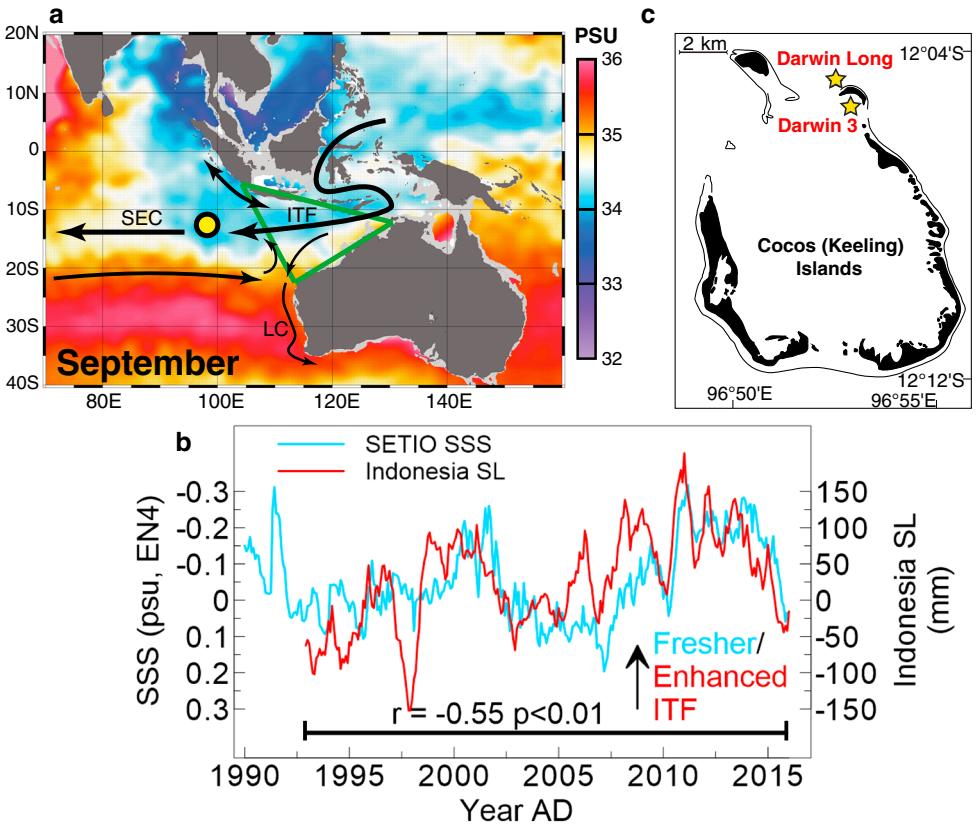

Figure 1. Sampling location, the observed SETIO hydrology and ITF. (a) Surface salinity (to 50 m) in the area of the Indonesian archipelago during September. The ITF and its derivatives, South Equatorial Current (SEC) and Leeuwin Current (LC), are indicated. The yellow dot indicates the location of Cocos (Keeling) Islands. The area within the green triangle delimits the Indo-Australian Basin. (b) Comparison of SETIO "EN 4" SSS (Good et al., 2013) (grid box 90–120°E, 5–25°S) and Indonesian sea level (Nerem et al., 2010, data used with permission) anomalies (monthly, relative to 1993–2007). Increased/decreased ITF transport is associated to higher/lower Indonesian sea level, respectively (Tillinger & Gordon, 2009; Wyrtki, 1987). The interval and correlation between the monthly anomaly data of SETIO SSS and Indonesian sea level are indicated in black. (c) Sample location on Cocos (Keeling) of the two coral cores (yellow stars) used in this study.

important baroclinic boundary that drives transport into the adjacent Indian Ocean (Andersson & Stigebrandt, 2005). Water that flows through the ITF accumulates in the Indo-Australian Basin during February–June (so-called "buffering"), before leaking into the SETIO area during the remainder of the year (Meyers, 1996; Phillips et al., 2005; Qu et al., 2008) (Figure 1a). Indonesian sea level covaries with ITF outflow (Tillinger & Gordon, 2009; Wyrtki, 1987), and the correlation between SETIO SSS and Indonesian sea level testifies to the dominant ITF control on regional SSS since at least 1993 when measurements started (Figure 1b). Hence, proxy records of past SETIO SSS can potentially be used to extend instrumental records of ITF and its leakage into the Indian Ocean.

We derived the surface ocean thermohaline conditions at Cocos using paired analyses of Sr/Ca and $\delta^{18}O$ from coral carbonate. Coral Sr/Ca is recognized as a skillful proxy of SST (Beck et al., 1992; Corrège, 2006; Marshall & McCulloch, 2001) and used here to remove temperature effects from the coral $\delta^{18}O$ to determine changes in seawater $\delta^{18}O$ ($\delta^{18}O_{sw}$) (Cahyarini et al., 2008; Ren et al., 2002), which can be linked to freshwater input/SSS (Bolton et al., 2014; Corrège, 2006; McCulloch et al., 1994; Nurhati et al., 2011). Cores "Darwin Long" (DL; dating back to 1808) and "Darwin 3" (D3; dating back to 1987) were drilled from *Porites* corals of the Cocos atoll (Figure 1c) and sampled with bimonthly resolution with strong chronological control. Especially the DL site is continuously flushed by ITF-derived oceanic waters (see Hua et al., 2004, 2005) and well outside the reach of stagnant lagoonal waters and thus suitable to deduce ITF-controlled changes in SETIO hydrological conditions over the last two centuries.

2. Pacific and Indian Ocean Climate Modes and ITF Transport Into the Indian Ocean

ITF transport is driven by the sea level pressure gradient between the Pacific and Indian Oceans (Wyrtki, 1987), which itself is controlled by zonal winds (Walker circulation) (e.g., Liu et al., 2015) as well as buoyancy variability (i.e., temperature and salinity variations) (Hu & Sprintall, 2016, 2017). The primary interannual climate modes of the Pacific Ocean (El Niño—Southern Oscillation; ENSO) and Indian Ocean (Indian Ocean Dipole; IOD) strongly affect the zonal equatorial winds, and hence, their covarying nature often causes an opposing effect on ITF leakage into the South Equatorial Current (SEC) as part of the global ocean circulation (Liu et al., 2015). ITF transport itself is found to be dominantly controlled by ENSO (Meyers, 1996; Tillinger & Gordon, 2010; van Sebille et al., 2014), while buffering of ITF-derived surface water in the Indo-Australian Basin is strongly regulated by the prevailing winds in the Indian Ocean and thus IOD (Liu et al., 2015; Qu et al., 2008). The buoyancy component that affects ITF transport typically reinforces the zonal wind component, as freshening due to increased rainfall in the Indonesian Seas increases ITF transport during La Niña conditions, and vice versa occurs during El Niño conditions (Du et al., 2015; Hu & Sprintall, 2016, 2017). Multidecadal trends in equatorial Pacific winds have been linked to Pacific decadal climate variability, such as represented by the Pacific Decadal Oscillation (PDO) (Mantua & Hare, 2002; Newman et al., 2016). The recent (1993) trend reversal of the ITF has been linked to a regime shift of the PDO (Feng et al., 2011), but long time scale data on ITF leakage into the SEC are missing to ascertain a longer term link.

3. Materials and Methods

3.1. Coral Cores and Sampling

Samples from this study were acquired from the Cocos (Keeling) islands (12.087°S, 96.875°E, Figures 1a and 1c), which were surveyed by Charles Darwin in 1836. Coral cores from massive *Porites* corals, referred to as Darwin Long (DL in short, 5.8 m water depth) and Darwin 3 (D3 in short, 4.9 m water depth), were drilled vertically down the colonies' apex in February 2010 off Direction Island at the southern atoll of Cocos (Figure 1c). Prior to analysis the coral cores were sliced into 7 mm thick slabs and cleaned following the protocol using NaOCl and ultra-pure Milli-Q water (Nagtegaal et al., 2012). After cleaning, the coral cores were photographed under visible and UV light, using the AVAATECH core scanner to reveal luminescent growth banding (Grove et al., 2010). The UV-luminescence banding was used together with digitalized X-rays to deduce the orientation of the growth axis in the DL and D3 coral cores and determine the most suitable sampling transect (see Figures S1 and S2 in the supporting information).

A high-resolution sampling transect was drilled using a 0.9 mm diameter drill (Horico H164 009). This sampling regime was chosen to obtain ~6 samples per year, ~1.25–1.5 mm intervals, that is, bimonthly resolution. For the DL core this resulted in 1,227 samples. We used the D3 core as a shorter reference core to test the robustness of the geochemical variability in the DL core. From the D3 core we obtained 260 samples.

3.2. Sr/Ca Analyses and SST Reconstruction SETIO

Sr/Ca ratios were measured at Kiel University with a simultaneous inductively coupled plasma optical emission spectrometer (ICP-OES, Spectro Ciros CCD SOP). Approximately 0.5 mg of coral powder was dissolved in 1.00 mL 0.2 *M* HNO_3. Prior to analysis, this solution was diluted with 0.2 *M* HNO_3 to a final concentration of ~8 ppm. An in-house coral powder standard (Mayotte) was prepared in an analogous way and used as consistency standard, being reanalyzed after every six samples. Sr and Ca were measured at their 407 and 317 nm emission lines, respectively. Our intensity ratio calibration strategy combined the techniques described by Schrag (1999) and de Villiers et al. (2002). Analytical internal precision of Sr/Ca measurements was 0.007 mmol/mol (1σ) or 0.08% (relative standard deviation, RSD). The international reference material JCp-1 (coral powder) was analyzed with every sample batch ($N = 6$ in each run) to reveal external reproducibility, which was $<0.15\%$ (RSD) or 0.01 mmol/mol. The average Sr/Ca value of the JCp-1 standard from multiple measurements on the same day and on consecutive days was 8.820 mmol/mol, indicating an accuracy $<0.20\%$ relative to the average value (8.838 mmol/mol) reported in Hathorne et al. (2013).

The DL and D3 coral Sr/Ca proxy data were transformed into SETIO SST anomalies in °C following the approach of Zinke et al. (2015). In short, the DL Sr/Ca data were normalized to its variance (subtract mean and divide by standard deviation) using the time period of 1961–1990. Subsequently, this normalized DL Sr/Ca record was scaled to the standard deviation of the SETIO ERSSTv3b2 (Smith et al., 2008) SST (grid

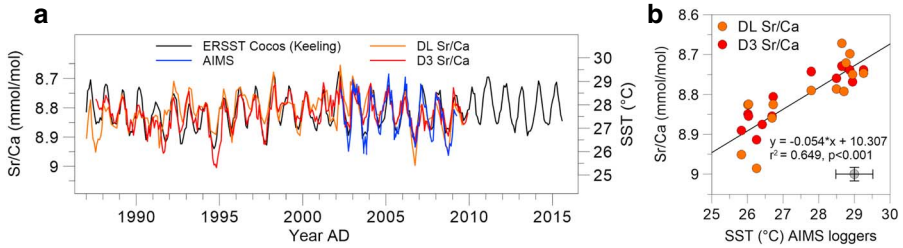

Figure 2. Coral Sr/Ca data and instrumental SST data for age model building and Sr/Ca calibration. (a) For age model construction Sr/Ca data from the coral cores were linked to the warmest month in the SST data from SST data loggers of the AIMS (blue) and ERSST (Smith et al., 2008) (black, grid box 95-97E, 11-13S), here exemplified for the interval from 1987 to 2009. The AIMS SST data from the different loggers were combined to form a composite record of local SST from 2002 to 2009 of the Cocos (Keeling) area. (b) Regression function of AIMS data logger SST minima and maxima to the Sr/Ca maxima and minima, respectively. The grey symbol in the lower right corner indicates the 2σ analytical error (Sr/Ca; vertical bar) and 2σ propagated error of Sr/Ca-derived SST (horizontal bar).

box 90–120°E, 25–5°S) for the same period of 1961–1990. The 95% confidence interval of the Sr/Ca-SST record was estimated by calculation of the maximum spread in the standard deviations of the SETIO ERSSTv3b2 that were used to scale the Sr/Ca record, also following Zinke et al. (2015). As the 1961–1990 period is missing for the D3 coral, we used the DL coral data to scale D3 Sr/Ca to SETIO SST from the ERSST v3b2 database. Bimonthly anomalies (relative to the 1961–1990 period) were calculated for the Sr/Ca-derived SST data of the DL and D3 corals. The D3 coral core lacks the time period of 1961–1990 (dating back to 1987), and hence, we used the mean data of the DL coral core to calculate anomalies for the D3 data.

3.3. Oxygen Isotope Analyses and Seawater δ^{18}O Reconstruction SETIO

The oxygen isotope (δ^{18}O) analyses were carried out on the same samples used for Sr/Ca analyses, using a Kiel IV carbonate preparation device coupled to a Finnigan MAT 253 mass spectrometer at the Royal NIOZ, Netherlands. Repeated analyses of the international standard NBS-19 showed a standard deviation of $<$0.07‰ for δ^{18}O. All δ^{18}O values are reported in per mil after normalization to the Vienna Pee Dee Belemnite isotope scale (‰ VPDB).

We used the approach of Ren et al. (2002) to remove the thermal effect on instantaneous changes of coral δ^{18}O by using the instantaneous changes in (Sr/Ca-derived) SST for both DL and D3 corals. In order to transfer the Sr/Ca changes in mmol/mol to local SST changes in °C, we regressed the minima and maxima in DL coral Sr/Ca to in situ SST measurements by the Australian Institute of Marine Science (AIMS) data loggers (Figure 2b). This yielded a slope of $-$0.0544 mmol/mol per 1°C, well in agreement with published slopes (Corrège, 2006). This slope was subsequently used to calculate Sr/Ca-based changes in °C, and converted into the thermal component of δ^{18}O changes using a coral δ^{18}O-SST relationship of $-$0.2‰ per 1°C (Juillet-Leclerc & Schmidt, 2001). These SST-related δ^{18}O changes were then subtracted from the instantaneous changes of coral δ^{18}O to produce the $\delta^{18}O_{sw}$ changes.

Bimonthly anomalies (relative to the 1961–1990 period) were calculated for the δ^{18}O and $\delta^{18}O_{sw}$ data of the DL and D3 corals. Similarly as for the Sr/Ca data, we used the mean data of the DL coral core to calculate anomalies for the D3 data. The average D3 δ^{18}O value over the 1987–2009 period was more negative than that of the DL core ($-$0.29‰ for δ^{18}O), potentially due to the location of D3 within the lagoon being more susceptible to local freshwater and/or higher SSTs by increased warming of the shallower lagoon water (Figure 1c). For analyzing the multiannual variability in $\delta^{18}O_{sw}$ in both records we centered the D3 data on the DL data (subtract $-$0.29‰) to show that the overall variability is similar in both cores.

The estimated uncertainty displayed for $\delta^{18}O_{sw}$ is calculated following Nurhati et al. (2011). The regression of Sr/Ca to AIMS SST took into account (i) the analytical precision of the Sr/Ca measurements (±0.16°C, 1σ) derived from multiple measurements of JCP-1 standard and (ii) a Sr/Ca-SST regression calibration slope error (± 0.21°C, 1σ). Subsequently, for calculation of the error on $\delta^{18}O_{sw}$, the terms (i) and (ii) were taken into account, formulated as promille (±0.03‰ and ±0.04‰, respectively), and also including (iii) the δ^{18}O-SST regression calibration slope error (±0.02‰, 1σ) (Juillet-Leclerc & Schmidt, 2001), and (iv) analytical error in

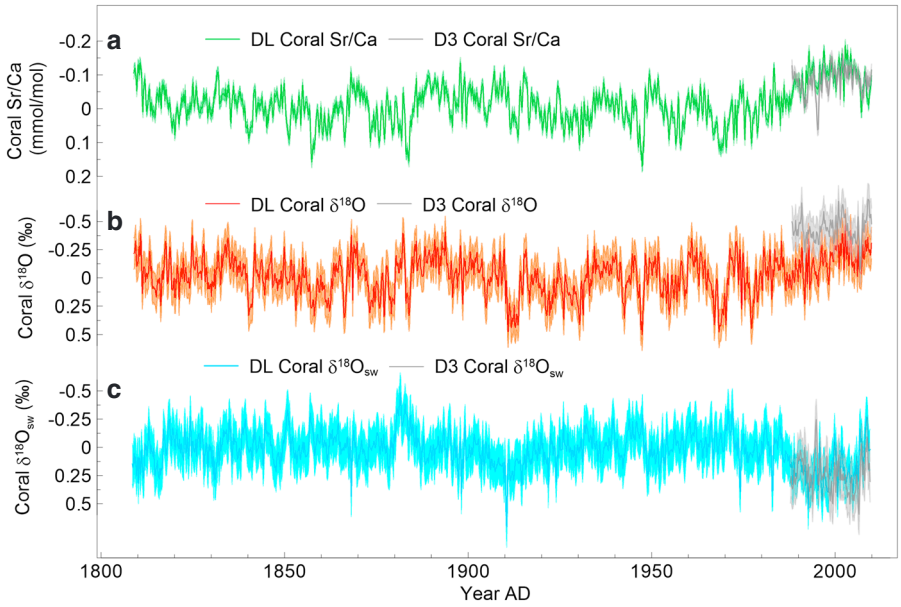

Figure 3. Coral-derived Sr/Ca, $\delta^{18}O$, and $\delta^{18}O_{sw}$ data from Cocos. (a) Sr/Ca of the DL and D3 corals. (b) $\delta^{18}O$ of the DL and D3 corals. (c) Calculated $\delta^{18}O_{sw}$ values for DL and D3 corals (D3 is centered at DL; see section 3.3). Data shown as bimonthly anomalies relative to the 1961–1990 (mean data of the DL coral core is used to calculate anomalies for the D3 data). The shadings indicate 2σ (analytical) uncertainties.

$\delta^{18}O$ measurements (±0.07‰, 1σ), derived from multiple measurements of NBS-19 standard. Ultimately, the terms (i)–(iv) were quadratically combined, leading to an 2σ error estimate of ±0.18‰ for the $\delta^{18}O_{sw}$ measurements.

3.4. Coral Core Chronology

The pronounced seasonal cycle in Sr/Ca (i.e., SST) was used to develop a chronological framework for each coral core (exemplified in Figure 2a). We assigned the lowest Sr/Ca value of each cycle to the warmest month provided by a composite record of local, in situ, monthly resolved SST data from data loggers of AIMS, and SST data from ERSSTv3b2 (Smith et al., 2008) (set to a grid box of 95–97°E, 11–13°S). The AIMS data were used to construct the age model from 2009 to 2002. The ERSST was used to construct the age model from 2002 to 1854. Prior to 1854 we assigned March, the warmest month on average, to the lowest Sr/Ca values of each seasonal cycle. The year-to-year variability of the occurrence of the warmest month varied by about 1–2 months between 1854 and present; thus, the added estimated age uncertainty is ~1–2 months prior to 1854. The Sr/Ca-based time series were linearly interpolated to a bimonthly resolution using the Analyseries software package (Paillard et al., 1996). The longest DL coral core spans a period of 201 years and dates back to 1808. The shorter D3 coral core dates back to 1987.

3.5. Climate Data

The shown PDO, ENSO (NINO3.4 Index), and IOD (DMI Index) indices are all based on ERSST v3b2 data (Smith et al., 2008). The GMST data, based on observational data, were downloaded from www.ncdc.noaa.gov/cag/time-series/global and from http://berkeleyearth.org/data/. The proxy data for the West Atlantic, West Pacific, and Indian Ocean were published in Tierney et al. (2015), which combined multiple data sets of Sr/Ca and $\delta^{18}O$ from tropical corals to make robust reconstructions of SST in these regions over the past four centuries. The tropical SST reconstructions covered the tropical Indian (20°N–15°S, 40–100°E), Western Pacific-Southeast Indian (25°N–25°S, 110–155°E), and Western Atlantic (15–30°N, 60–90°W) Oceans. Also the Eastern Pacific was reconstructed, but this record was found to contain large uncertainty (Tierney et al., 2015), and therefore, we refrain from showing this record. The data of 20th century Pacific trade winds, obtained from Pacific coral Mn/Ca, were published by Thompson et al. (2015).

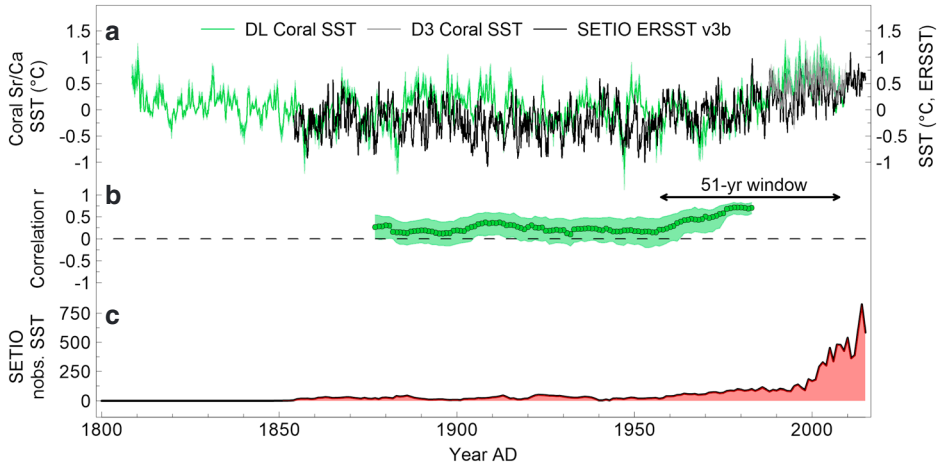

Figure 4. Coral-derived Sr/Ca SST data for the SETIO and instrumental SST data. (a) Comparison of bimonthly anomalies (1961–1990) for Sr/Ca-based SST from DL and D3 corals (the shadings indicate 95% confidence intervals) and monthly anomalies (1961–1990) of SETIO ERSSTv3b2 (Smith et al., 2008) SST (grid box 90–120°E, 5–25°S). (b) Running correlation (51 year window) between the annually averaged records of DL Sr/Ca SST to ERSST SST from the SETIO region (green dots, the shadings indicate 95% confidence intervals). (c) The number of ICOADS v2.5 SST observations (Woodruff et al., 2011) in the SETIO area (grid box 90–120°E, 5–25°S) per year, which are used to compute the ERSST SST data. Figure S3 provides a zoom in on the interval from 1950 to 2015, while Figure S4 shows the same data relative to the SETIO HadISST SST (Rayner et al., 2003).

3.6. Spectral Analyses and Spatial/Running Correlations

The conducted REDFIT spectral analyses (Schulz & Mudelsee, 2002) were performed with the PAST software package (Hammer et al., 2001). REDFIT spectral analyses were performed with an oversampling factor of 4 (controlling number of data points on frequency axis), 4 "Welch overlapped segments" (overlapping by 50%, for noise reduction), and a χ^2 test for indication of the 90% and 95% "false-alarm" lines.

The spatial and running correlations (with their 95% confidence intervals) between the variable records were computed using KNMI Climate Explorer (http://climexp.knmi.nl) (van Oldenborgh & Burgers, 2005). Before the running correlations were performed the bimonthly anomaly data were converted into annual means (January–December). The running correlations in Figures 6 and 9 were also linearly detrended, within Climate Explorer, to focus on interannual to multidecadal variability. Detrending removes potential spurious correlations due to long-term linear trends, which may be shared between two time series.

4. Results and Discussion

4.1. SETIO Instrumental Hydrological Data and Coral-Derived Sr/Ca, $\delta^{18}O$ and $\delta^{18}O_{sw}$

The Sr/Ca records from the DL and D3 corals show similar results (Figure 3a), indicating a consistent and robust SST signal ($r = 0.50$; $p < 0.01$; Table S1 in the supporting information) in both records. The DL SST record derived from Sr/Ca concurs well with observational SETIO SSTs from the ERSST database (Smith et al., 2008) (Figure 4; Figure S4 shows the same data relative to the SETIO HadISST; Rayner et al., 2003), showing particularly high correlations since ~1960 when the number of observations increased (max $r = 0.71$, $p < 0.01$) (Figures 4b and 4c). This concurs with the high spatial correlation of annual, detrended (hence focused on interannual variability) Sr/Ca-derived and instrumental ERSST data within the SETIO area (Figure 5; Figure S5 shows the same data relative to the SETIO HadISST; Rayner et al., 2003). This confirms the skill of Sr/Ca to capture SST variability for not only Cocos, but for the whole SETIO region.

For the DL coral, 57% of the variance in $\delta^{18}O$ is explained by Sr/Ca-derived SST (Figures 3a and 3b), leaving the remainder potentially determined by $\delta^{18}O_{sw}$ (Figure 3c), which, in turn, is often associated to salinity (Corrège, 2006; McCulloch et al., 1994). The calculated $\delta^{18}O_{sw}$ for the DL and D3 coral cores show similar variability over the common length of the records ($r = 0.55$, $p = 0.01$; Figure 6a), emphasizing the consistency of Cocos coral-derived $\delta^{18}O_{sw}$. Comparison between the calculated DL $\delta^{18}O_{sw}$ and observational SETIO SSS data from the "EN4" database (Good et al., 2013) (Figure 6b) shows low correlations prior to the 1980s and

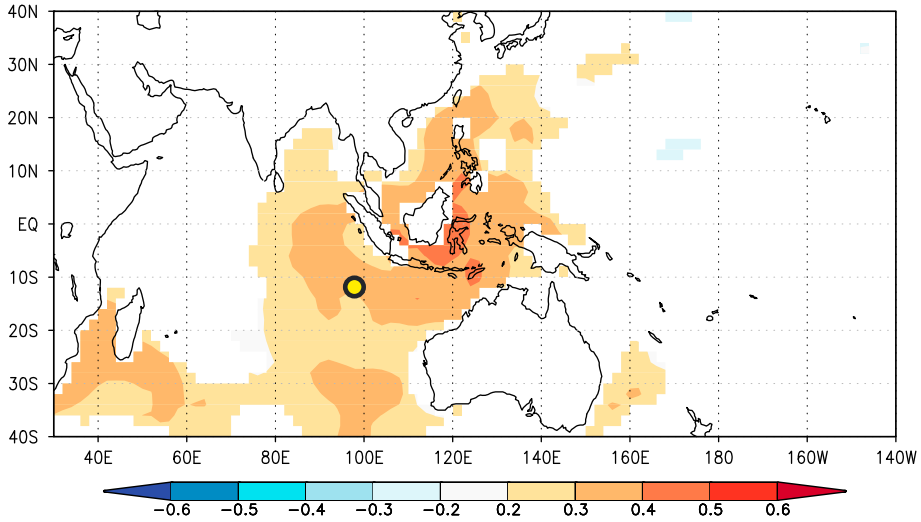

Figure 5. Spatial correlation ($p < 0.05$) of DL coral Sr/Ca SST to instrumental SST data from ERSSTv3b2 (Smith et al., 2008) (January–December averaged data, detrended, with overlapping period of 1854–2008). The yellow dot indicates the location of Cocos (Keeling) Islands. Similarly, Figure S5 shows the spatial correlation between the DL coral Sr/Ca SST to the SETIO HadISST SST (Rayner et al., 2003).

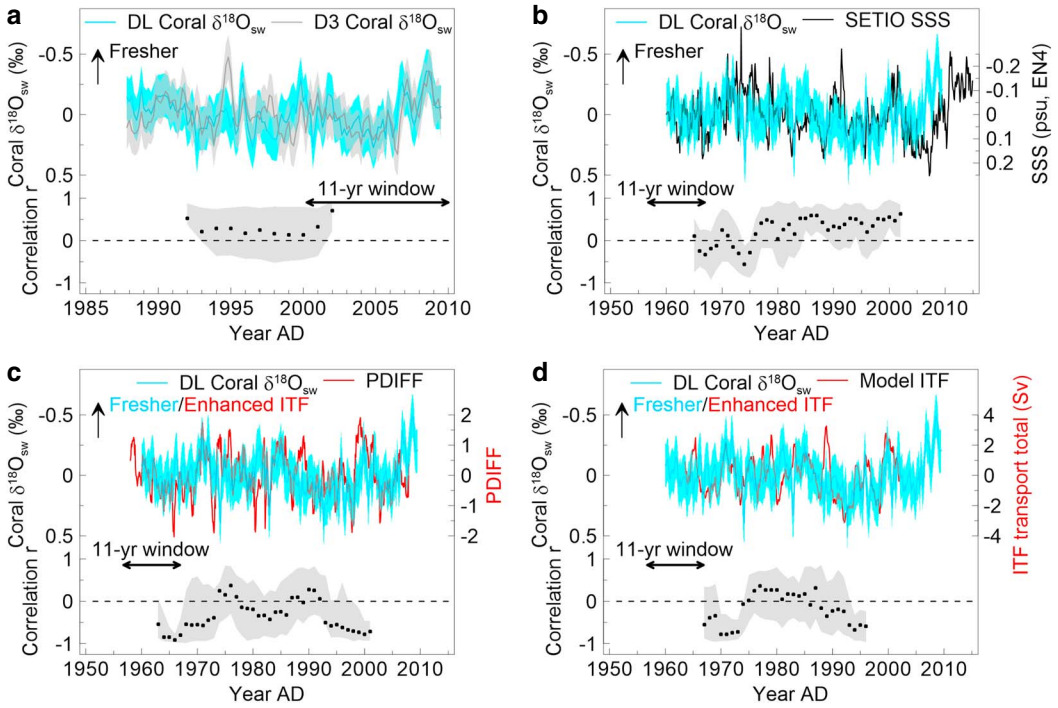

Figure 6. Coral-derived $\delta^{18}O_{sw}$ data and instrumental/model data for SSS and ITF transport. (a) Comparison of detrended bimonthly anomaly data (centered) of DL to D3 $\delta^{18}O_{sw}$ (the shadings indicate 2σ uncertainties). The bottom shows an 11 year window running correlation (black dots, 95% confidence intervals in grey) between annual detrended data of the records with an overlapping period from 1987 to 2009. (b) Same as Figure 6a, but comparing detrended bimonthly anomalies of DL $\delta^{18}O_{sw}$ to monthly SETIO SSS anomalies from the EN4 database (Good et al., 2013) with an overlapping period from 1960 to 2009. (c) Same as Figure 6a, but comparing bimonthly detrended anomalies of DL $\delta^{18}O_{sw}$ to the Pacific-Indian Ocean pressure difference (PDIFF) (Tillinger & Gordon, 2009) with an overlapping period from 1958 to 2007. (d) Same as Figure 6a, but comparing detrended bimonthly anomalies of DL $\delta^{18}O_{sw}$ to full transport of modeled Lagrangian ITF (van Sebille et al., 2014) with an overlapping period from 1963 to 2002.

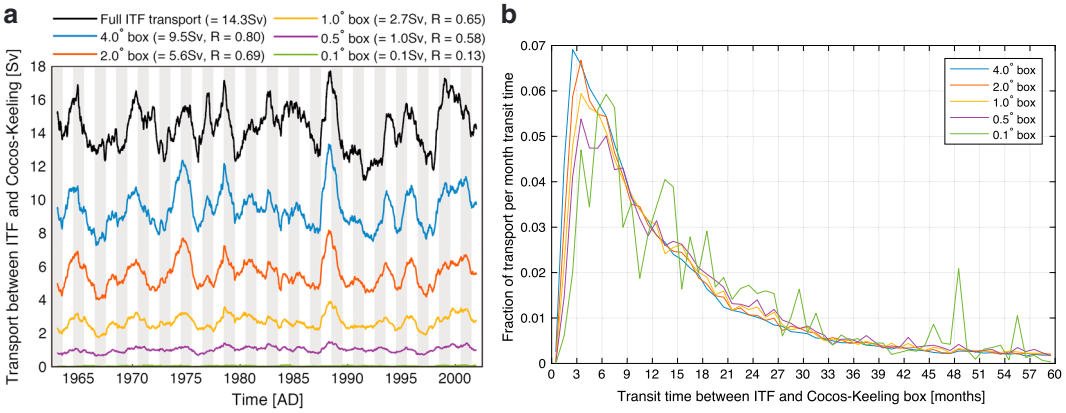

Figure 7. Modeled time series of Lagrangian Indonesian throughflow toward Cocos (Keeling). (a) Lagrangian ITF with a 1 year moving average smoothing applied, for the full transport (black) (van Sebille et al., 2014) and transport that ends in defined grid boxes around Cocos (see legend). (b) Transit times of the virtual Lagrangian particles to arrive from the ITF region in grid boxes around Cocos.

increasingly higher positive correlations afterward, when instrumental data coverage and precision in EN4 improve (Du et al., 2015). Coral-derived $\delta^{18}O_{sw}$ is hence likely a consistent recorder of large-scale advective processes in SETIO SSS, with the "EN4" database deviating further back in time when observations become increasingly sparse. Comparison between the DL $\delta^{18}O_{sw}$ and observational SETIO SSS data from the Simple Ocean Data Assimilation database (Carton & Giese, 2008) shows a consistent positive correlation (Figure S6), also highlighting the skill of DL $\delta^{18}O_{sw}$ to capture variability in SETIO SSS.

4.2. ITF Control on SETIO SSS and Seawater $\delta^{18}O$

We first assessed the ITF transport toward the coral site over the last 50 years by an eddy-permitting ocean model simulation with virtual Lagrangian particles (detailed methodology in van Sebille et al., 2014). This model approach showed that the waters reaching the region around Cocos (4° × 4° and smaller box sizes) are to large extend derived from the ITF (Figure 7a), generally within 3 to 9 months after passing Indonesia (Figure 7b). Lower correlations at subgrid scale between full ITF transport and the transport reaching Cocos (Figure 7a) are possibly due to an increased model uncertainty as the subgrid-scale diffusivity needs to be taken into account. Nonetheless, in line with the $\Delta^{14}C$ values of Cocos *Porites* showing an ITF signature (Hua et al., 2004, 2005), our modeled results point toward a direct impact of the ITF on thermohaline surface water conditions at Cocos.

Running correlations between detrended, annual $\delta^{18}O_{sw}$ and the Pacific-Indian Ocean pressure difference (PDIFF) (Tillinger & Gordon, 2009) show mostly negative correlations ($r = -0.35$, $p < 0.05$ for the entire common interval) (Figure 6c). This demonstrates that indeed SSS freshens at Cocos during stronger ITF intervals, in accordance with observational data (Feng et al., 2015; Phillips et al., 2005). Similarly, coral $\delta^{18}O_{sw}$ is also significantly correlated to total ITF transport deduced from Lagrangian modeling (van Sebille et al., 2014)

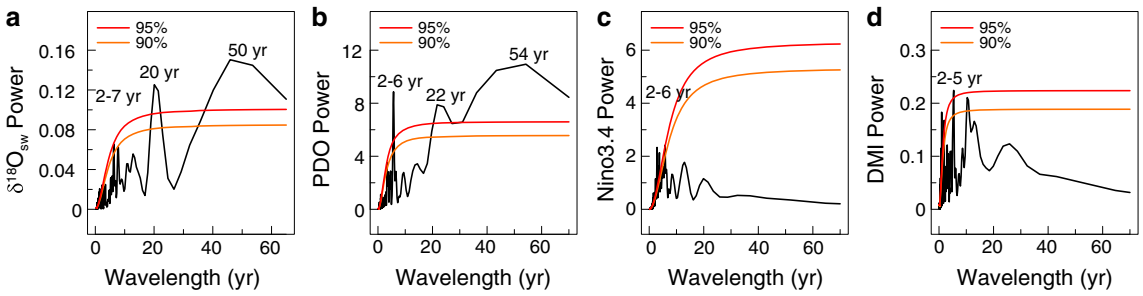

Figure 8. (a) REDFIT analyses performed on detrended bimonthly anomalies (1961–1990) of Cocos DL coral $\delta^{18}O_{sw}$ (b-d) REDFIT analyses performed on detrended monthly anomalies (1961–1990) of the climate indices for PDO, ENSO, and IOD, respectively.

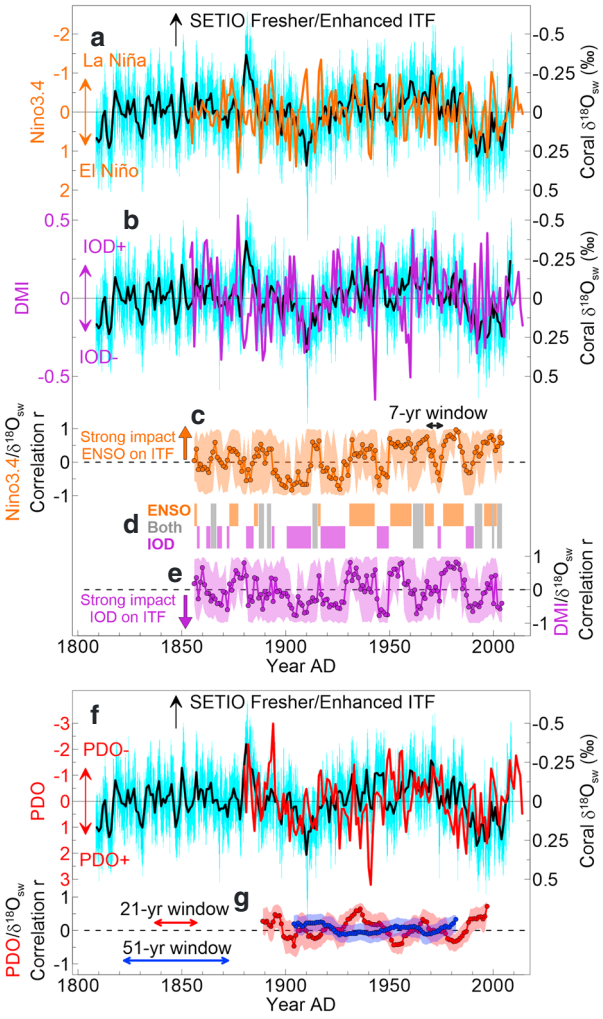

Figure 9. Comparison of Cocos coral $\delta^{18}O_{sw}$ and Pacific and Indian Ocean climate modes. The detrended annual values for (a) ENSO (orange), (b) IOD (purple), and (f) PDO (red) climate indices compared to detrended annual data of $\delta^{18}O_{sw}$ (black; bimonthly detrended data with 2σ confidence intervals in blue). The running correlations between the (c, e, and g) climate indices and $\delta^{18}O_{sw}$ have windows adjusted to the dominant frequencies within the climate modes (the shadings indicate the 95% confidence intervals). The intervals that ENSO (orange), IOD (purple), or both (grey) mainly affect the SETIO SSS are marked in Figure 9d.

($r = -0.40$, $p < 0.05$) (Figure 6d). This correlation is quite similar to the value found between SETIO SSS and Indonesian sea level ($r = -0.55$, $p < 0.01$; Figure 1b). The ITF leakage recorded in Cocos $\delta^{18}O_{sw}$ is thus largely regulated by the ITF strength during the time interval overlapping with reanalysis data. Therefore, Cocos $\delta^{18}O_{sw}$ is potentially suited to reconstruct ITF-controlled hydrological conditions in the SETIO region over the past 200 years. Nevertheless, temporally weakened correlations between ITF and $\delta^{18}O_{sw}$ suggest that the regional precipitation-evaporation balance and meridional advective processes may attenuate the ITF leakage recorded in Cocos $\delta^{18}O_{sw}$.

4.3. Interannual to Multidecadal Climate Forcing of SETIO SSS

We assessed the multidecadal variability in ITF leakage into the Indian Ocean by performing REDFIT spectral analysis (Schulz & Mudelsee, 2002) on Cocos coral $\delta^{18}O_{sw}$, which showed highly significant peaks in 2 to 7 year, 20 year, and 50 year bands (Figure 8a). The decadal variability in the 20 year and 50 year domains is highly indicative of Pacific decadal climate variability, represented by the PDO (Mantua & Hare, 2002; Newman et al., 2016) (Figure 8b). The 2–7 year cycles can be linked to ENSO (NINO3.4 Index) and/or IOD (Dipole Mode Index, DMI) variability (Figures 8c and 8d), which are both known to highly influence ITF leakage into the Indian Ocean on shorter interannual time scales (Liu et al., 2015; Tillinger & Gordon, 2009; van Sebille et al., 2014).

On interannual time scales, running correlations indicate a highly variable impact of ENSO (Figures 9a and 9c) and/or IOD (Figures 9b and 9e) on SSS conditions in the Cocos Islands with decades of positive and decades of negative correlation during the past 150 years (Figure 9d). Observations show that El Niño/La Niña causes lower/higher ITF transport, respectively, while IOD−/IOD+ causes lower/higher ITF leakage, respectively (Liu et al., 2015; Meyers, 1996; Qu et al., 2008; Sprintall & Révelard, 2014). This often results in an opposing effect of the Pacific-Indian Ocean climate modes on ITF transport, as El Niño/La Niña generally co-occurs with IOD+/IOD−, respectively (Liu et al., 2015). We infer, based on the observations, that a positive correlation between NINO3.4 and $\delta^{18}O_{sw}$ is expected when ENSO has a relative strong effect on SETIO SSS (Figure 9c) and that a negative correlation between DMI and $\delta^{18}O_{sw}$ is expected when IOD has a relative strong effect on SETIO SSS (Figure 9e). Our data suggest an alternating dominance of ENSO and IOD on ITF leakage during the last 150 years, with ENSO showing a stronger influence during the last 80 years (orange intervals in Figure 9d), in line with what we observe at present (Liu et al., 2015; Meyers, 1996), but the IOD appears more important for interannual variability in ITF leakage in the early 20th century (purple intervals in Figure 9d). The Pacific trade winds were found to be relatively weak from especially 1910 to 1930 (Thompson et al., 2015), and we speculate that this is associated to the increased impact of the IOD on ITF leakage into the Indian Ocean during those times.

On multidecadal time scales spectral analysis suggests a potential impact of the PDO on SETIO SSS. The running correlations between PDO and Cocos $\delta^{18}O_{sw}$ show relatively modest (generally positive) correlations during the interval that they overlap (Figures 9f and 9g), possibly due to the much larger impact of interannual climate variability (Figures 9a–9e). Nonetheless, the impact of the PDO on ITF transport can be exemplified by focusing on well-known PDO regime shifts (Newman et al., 2016), especially when compared to a smoothed (15 year moving averaged) Cocos $\delta^{18}O_{sw}$ record (Figure 10a). The dominant PDO states from ~1947 to 1976 (PDO−), ~1977 to 1998 (PDO+), and ~1999 to present (PDO−) relate to (on average), respectively, fresher, saltier, and again fresher conditions in the SETIO region as deduced from Cocos $\delta^{18}O_{sw}$. A slowdown of the ITF and SEC has been observed for specifically the regime shift at ~1977

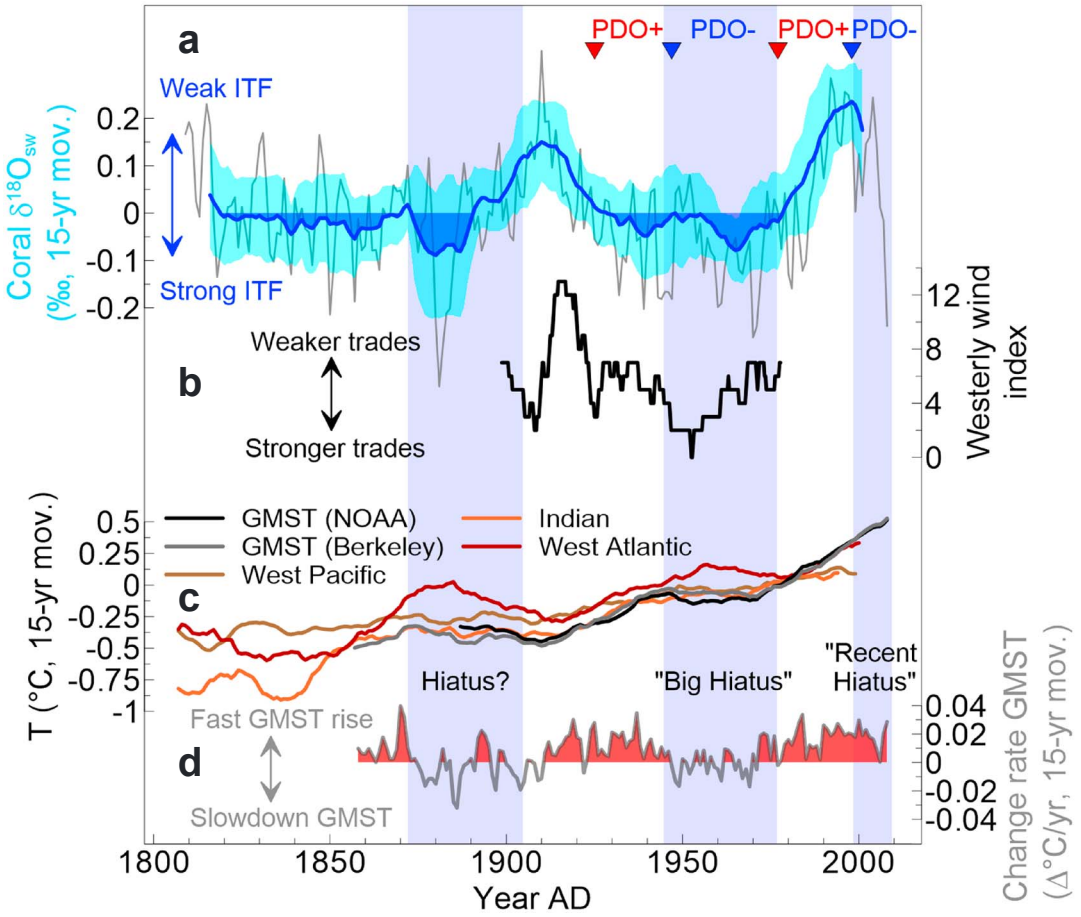

Figure 10. SETIO SSS (and ITF leakage) from Cocos corals and GMST. (a) 15 year moving averaged anomaly (1961–1990) of Cocos DL coral $\delta^{18}O_{sw}$ (the shading is 15 year moving standard deviation; the grey color shows annual data of $\delta^{18}O_{sw}$). The triangles show well-known regime shifts of the PDO toward PDO+ (red) and PDO− (blue) states (Newman et al., 2016). (b) Coral-based Pacific trade winds index (Thompson et al., 2015). (c) The 15 year moving averaged anomalies (1961–1990) of GMST and proxy-based ocean temperature (from the West Pacific (including SETIO), West Atlantic, and tropical Indian Oceans) (Tierney et al., 2015). (d) The 15 year moving averaged anomaly (1961–1990) of year-to-year rate of change in the Berkeley GMST record. The blue background shadings in the figure indicate potential intervals of slowed GMST rise.

toward PDO+ (Wainwright et al., 2008). The return to lower surface salinities in the SETIO from mid-1990s to 2000s also appears in instrumental records and is thought to result from a sharp climatic regime shift of the PDO (Du et al., 2015; Feng et al., 2011, 2015). The dominant PDO state from 1925 to 1946 (PDO+) would favor saltier conditions but appears concurrent with fresher SETIO SSS (increased ITF leakage) as derived from coral $\delta^{18}O_{sw}$. Several La Niñas occurred around that time, suggesting that the PDO affects ITF leakage but is still in competition with interannual climate modes.

The PDO likely impacts SETIO SSS by modifying the easterly winds over the equatorial Pacific, as also observed in the mid-1970s and mid-1990s (Du et al., 2015; Feng et al., 2011). The high correspondence between ITF-controlled Cocos $\delta^{18}O_{sw}$ and Pacific trade winds supports this connection (Figures 10a and 10b). These results confirm the observed correlation between tropical Pacific trade winds and Western Australian sea level variability linked via the ITF and Leeuwin Current (Feng et al., 2004). A negative PDO state, similar to a La Niña event (Du et al., 2015), strengthens trade winds in the tropical Pacific. This likely increases ITF strength, in at least the upper 150 m of the water column (Sprintall & Révelard, 2014), by increasing sea level pressure gradients. Simultaneously, strengthened tropical Pacific trade winds enhance precipitation in the Indonesian archipelago (emphasizing the imprint on surface $\delta^{18}O_{sw}$), which strengthens the ITF even more through the halosteric component of ITF transport (see Hu & Sprintall, 2017). These conditions are reversed for a positive PDO state.

4.4. Multidecadal Variability in ITF and Rate of GMST Warming

Our results suggest that, in general, negative/positive PDO regime shifts enhance/reduce ITF leakage at least since ~1880. The rate of GMST warming varied on multidecadal time scales during the last century and Pacific decadal climate variability (PDO) has been found to be crucial for variability in GMST warming rates (Kosaka & Xie, 2016; Lee et al., 2015; Nieves et al., 2015; Trenberth, 2015; Trenberth & Fasullo, 2013). For the recent slowdown of GMST warming (~1998–2013) significant heat was removed from the Pacific Ocean surface (Trenberth, 2015; Trenberth & Fasullo, 2013), which has been linked to increased heat transport to the Indian Ocean via the ITF (Lee et al., 2015). A comparison between the 15 year trends in ITF leakage and rate of GMST change (Figure 10) suggests relatively enhanced ITF leakage during at least the so-called "Big Hiatus" (~1943–1975) and potentially pre-1906. The latter "hiatus" is indicated through the plateau in the warming rate during the last three decennia of the 19th century in the Berkeley GMST record (Figures 10c and 10d) and in multiproxy-SST records from the West Pacific, tropical Indian, and West Atlantic Oceans (Tierney et al., 2015) (Figure 10c), which line up with a higher ITF leakage from ~1872 to 1900 (Figure 10a). Hence, our results suggest that heat redistribution from the surface Pacific Ocean via the ITF to other ocean basins appears not restricted to the recent 1998–2013 interval alone. Moreover, ITF leakage weakened at ~1900–1930, concurrent with the start of the severe GMST warming acceleration from ~1906 to 1942, while the ITF also significantly weakened in ~1976–1997 when GMST warming accelerated.

The rate of GMST change has been linked to tropical Pacific wind strength (Thompson et al., 2015) (Figure 10b), and its effect on the ITF offers an additional mechanism to carry large quantities of surface heat from the Pacific into the Indian Ocean causing intervals where GMST warming slows down. This corroborates the net cooling in the surface Pacific Ocean that is observed during these times (Trenberth & Fasullo, 2013). In contrast, weakening of the Pacific trade winds and the ITF transport locks the surface heat inside the Pacific Ocean causing GMST rise to accelerate. As the interannual and multidecadal climate modes of the Pacific ultimately drive the variability in Pacific trade wind strength (England et al., 2014), these can be seen as the important pacemakers of GMST warming rate, in line with earlier research (see Trenberth, 2015).

5. Conclusions

The corals from the Cocos (Keeling) Islands offer a unique look into how the ITF impacted the surface hydrological conditions in the SETIO region over the last two centuries, thereby revealing important information on long-term (multidecadal) ITF variability. We find, in line with observational data, that interannual climate modes from the Pacific and Indian Ocean strongly affect ITF leakage into the SETIO region, probably through their effect on Pacific and Indian Ocean trade wind strength. From spectral analyses and running correlations we infer that the Pacific decadal climate variability (i.e., PDO) leaves a relative (compared to interannual climate modes) weaker but still consistent, imprint on ITF-controlled SETIO SSS over the past 200 years. Similar to interannual climate variability, the Pacific decadal climate variability likely modulates the ITF through changing the Pacific trade wind strength. The chain of physical processes behind Pacific decadal climate variability remains poorly understood (Newman et al., 2016), and modeling its evolution in the 21st century remains uncertain (Christensen et al., 2013). Our results suggest, however, that Pacific decadal climate variability is paramount for ITF transport variability and leakage into SEC. Pacific decadal climate variability is often seen as an important pacemaker of GMST warming, and our data suggest that intervals of ITF increase/decrease can generally be linked to global warming rate slowdown/acceleration. Therefore, we infer that heat redistribution through the ITF, driven through Pacific decadal climate variability, provides a consistent mechanism to modulate global climate. Additional proxy records of SST/SSS from the ITF exit region and long-term measurements of the ITF leakage properties are necessary to confirm the link between GMST and ITF strength, as inferred from our data.

Acknowledgments
We acknowledge the constructive comments by three anonymous reviewers, which were helpful to improve the original manuscript. We thank the VPRO, Royal NIOZ, and NWO for funding the coral drilling campaign as part of the Beagle program during the Darwin year (2009) and the people of Cocos Keeling Islands for assistance throughout the fieldwork and help with permits. We thank Gerrit van den Bergh (University of Wollongong) and Roel Nagtegaal for their help during retrieval and initial analysis of the coral cores. UV-luminescence analysis was supported through the SCAN2 program (NWO project 834.11.003). Analytical assistance of Piet van Gaever during oxygen isotope analyses was greatly appreciated. We thank Dieter Garbe-Schönberg from the Chistian Albrechts University Kiel (Germany) for assistance with the ICP-OES measurements and quality checks. Bouke Lacet and Wynanda Koot (VU University Amsterdam) helped cut the core slabs. The TROPAC01 model was developed within the framework of the DFG project SFB754 and integrated at the North-German Supercomputing Alliance (HLRN). EvS was supported by the Australian Research Council via grant DE130101336. A Senior Curtin Fellowship in Western Australia and an Honorary Fellowship with the University of the Witwatersrand in South Africa supported J.Z. R.H. is supported through NWO open competition project "SCANALOGUE" (ALWOP.2015.113). This work was partly carried out under the program of Netherlands Earth System Science Centre (NESSC), financially supported by the Dutch Ministry of Education, Culture and Science (OCW). The published data are archived in the PANGAEA data repository (https://doi.pangaea.de/10.1594/PANGAEA.883837).

References

Andersson, H. C., & Stigebrandt, A. (2005). Regulation of the Indonesian throughflow by baroclinic draining of the North Australian Basin. *Deep Sea Research Part I: Oceanographic Research Papers*, *52*(12), 2214–2233.

Beck, J. W., Edwards, R. L., Ito, E., Taylor, F. W., Recy, J., Rougerie, F., … Henin, C. (1992). Sea-surface temperature from coral skeletal strontium/calcium ratios. *Science*, *257*, 644–648.

Bolton, A., Goodkin, N., Hughen, K., Ostermann, D., Vo, S., & Phan, H. (2014). Paired Porites coral Sr/Ca and $\delta^{18}O$ from the western South China Sea: Proxy calibration of sea surface temperature and precipitation. *Palaeogeography, Palaeoclimatology, Palaeoecology*, *410*, 233–243.

Cahyarini, S. Y., Pfeiffer, M., Timm, O., Dullo, W.-C., & Schönberg, D. G. (2008). Reconstructing seawater δ18O from paired coral δ18O and Sr/Ca ratios: Methods, error analysis and problems, with examples from Tahiti (French Polynesia) and Timor (Indonesia). *Geochimica et Cosmochimica Acta*, *72*(12), 2841–2853.

Carton, J. A., & Giese, B. S. (2008). A reanalysis of ocean climate using Simple Ocean Data Assimilation (SODA). *Monthly Weather Review*, *136*, 2999–3017.

Christensen, J. H., Krishna Kumar, K., Aldrian, E., An, S.-I., Cavalcanti, I. F. A., de Castro, M., … Zhou, T. (2013). Climate phenomena and their relevance for future regional climate change. In by T. F. Stocker, et al. (Eds.), *Climate change 2013: The physical science basis. Contribution of Working Group I to the Fifth Assessment Report of the Intergovernmental Panel on Climate Change* (pp. 1217–1308). Cambridge, United Kingdom and New York, NY: Cambridge University Press.

Corrège, T. (2006). Sea surface temperature and salinity reconstruction from coral geochemical tracers. *Palaeogeography, Palaeoclimatology, Palaeoecology*, *232*(2), 408–428.

de Villiers, S., Greaves, M., & Elderfield, H. (2002). An intensity ratio calibration method for the accurate determination of Mg/Ca and Sr/Ca of marine carbonates by ICP-AES. *Geochemistry, Geophysics, Geosystems*, *3*(1), 1001. https://doi.org/10.1029/2001GC000169

Du, Y., Zhang, Y., Feng, M., Wang, T., Zhang, N., & Wijffels, S. (2015). Decadal trends of the upper ocean salinity in the tropical Indo-Pacific since mid-1990s. *Scientific Reports*, *5*, 16,050.

Durgadoo, J. V., Rühs, S., Biastoch, A., & Böning, C. W. (2017). Indian Ocean sources of Agulhas leakage. *Journal of Geophysical Research: Oceans*, *122*, 3481–3499. https://doi.org/10.1002/2016JC012676

England, M. H., McGregor, S., Spence, P., Meehl, G. A., Timmermann, A., Cai, W., … Santoso, A. (2014). Recent intensification of wind-driven circulation in the Pacific and the ongoing warming hiatus. *Nature Climate Change*, *4*, 222–227.

Feng, M., Benthuysen, J., Zhang, N., & Slawinski, D. (2015). Freshening anomalies in the Indonesian throughflow and impacts on the Leeuwin Current during 2010–2011. *Geophysical Research Letters*, *42*, 8555–8562. https://doi.org/10.1002/2015GL065848

Feng, M., Böning, C., Biastoch, A., Behrens, E., Weller, E., & Masumoto, Y. (2011). The reversal of the multi-decadal trends of the equatorial Pacific easterly winds, and the Indonesian throughflow and Leeuwin current transports. *Geophysical Research Letters*, *38*, L11604. https://doi.org/10.1029/2011GL047291

Feng, M., Li, Y., & Meyers, G. (2004). Multidecadal variations of Fremantle sea level: Footprint of climate variability in the tropical Pacific. *Geophysical Research Letters*, *31*, L16302. https://doi.org/10.1029/2004GL019947

Good, S. A., Martin, M. J., & Rayner, N. A. (2013). EN4: Quality controlled ocean temperature and salinity profiles and monthly objective analyses with uncertainty estimates. *Journal of Geophysical Research, Oceans*, *118*, 6704–6716. https://doi.org/10.1002/2013JC009067

Gordon, A. L. (1986). Interocean exchange of thermocline water. *Journal of Geophysical Research*, *91*(C9), 5037–5046.

Gordon, A. L., Susanto, R. D., & Ffield, A. (1999). Throughflow within Makassar Strait. *Geophysical Research Letters*, *26*(21), 3325–3328.

Grove, C. A., Nagtegaal, R., Zinke, J., Scheufen, T., Koster, B., Kasper, S., … Brummer, G. J. A. (2010). River runoff reconstructions from novel spectral luminescence scanning of massive coral skeletons. *Coral Reefs*, *29*(3), 579–591.

Hammer, Ø., Harper, D. A. T., & Ryan, P. D. (2001). Past: Paleontological statistics software package for education and data analysis. *Palaeontologia Electronica*, *4*(1), 9.

Hathorne, E. C., Gagnon, A., Felis, T., Adkins, J., Asami, R., Boer, W., … Douville, E. (2013). Interlaboratory study for coral Sr/Ca and other element/Ca ratio measurements. *Geochemistry, Geophysics, Geosystems*, *14*, 3730–3750. https://doi.org/10.1002/ggge.20230

Hu, S., & Sprintall, J. (2016). Interannual variability of the Indonesian throughflow: The salinity effect. *Journal of Geophysical Research: Oceans*, *121*, 2596–2615. https://doi.org/10.1002/2015JC011495

Hu, S., & Sprintall, J. (2017). Observed strengthening of interbasin exchange via the Indonesian seas due to rainfall intensification. *Geophysical Research Letters*, *44*, 1448–1456. https://doi.org/10.1002/2016GL072494

Hua, Q., Woodroffe, C. D., Barbetti, M., Smithers, S. G., Zoppi, U., & Fink, D. (2004). Marine reservoir correction for the Cocos (Keeling) Islands, Indian Ocean. *Radiocarbon*, *46*, 603–610.

Hua, Q., Woodroffe, C. D., Smithers, S. G., Barbetti, M., & Fink, D. (2005). Radiocarbon in corals from the Cocos (Keeling) Islands and implications for Indian Ocean circulation. *Geophysical Research Letters*, *32*, L21602. https://doi.org/10.1029/2005GL023882

Juillet-Leclerc, A., & Schmidt, G. (2001). A calibration of the oxygen isotope paleothermometer of coral aragonite from Porites. *Geophysical Research Letters*, *28*(21), 4135–4138.

Kosaka, Y., & Xie, S.-P. (2016). The tropical Pacific as a key pacemaker of the variable rates of global warming. *Nature Geoscience*, *9*(9), 669–673.

Le Bars, D., Dijkstra, H., & De Ruijter, W. (2013). Impact of the Indonesian throughflow on Agulhas leakage. *Ocean Science Discussions*, *10*, 353–391.

Lee, S.-K., Park, W., Baringer, M. O., Gordon, A. L., Huber, B., & Liu, Y. (2015). Pacific origin of the abrupt increase in Indian Ocean heat content during the warming hiatus. *Nature Geoscience*, *8*(6), 445–449.

Liu, Q. Y., Feng, M., Wang, D., & Wijffels, S. (2015). Interannual variability of the Indonesian throughflow transport: A revisit based on 30 year expendable bathythermograph data. *Journal of Geophysical Research: Oceans*, *120*, 8270–8282. https://doi.org/10.1002/2015JC011351

Mantua, N. J., & Hare, S. R. (2002). The Pacific Decadal Oscillation. *Journal of Oceanography*, *58*(1), 35–44.

Marshall, J. F., & McCulloch, M. T. (2001). Evidence of El Nino and the Indian Ocean Dipole from Sr/Ca derived SSTs for modern corals at Christmas Island, eastern Indian Ocean. *Geophysical Research Letters*, *28*(18), 3453–3456.

McCulloch, M. T., Gagan, M. K., Mortimer, G. E., Chivas, A. R., & Isdale, P. J. (1994). A high-resolution Sr/Ca and $\delta^{18}O$ coral record from the Great Barrier Reef, Australia, and the 1982–1983 El Nino. *Geochimica et Cosmochimica Acta*, *58*(12), 2747–2754.

Meyers, G. (1996). Variation of Indonesian throughflow and the El Niño—Southern Oscillation. *Journal of Geophysical Research*, *101*(C5), 12,255–12,263.

Nagtegaal, R., Grove, C. A., Kasper, S., Zinke, J., Boer, W., & Brummer, G.-J. A. (2012). Spectral luminescence and geochemistry of coral aragonite: Effects of whole-core treatment. *Chemical Geology*, *318*, 6–15.

Nerem, R., Chambers, D., Choe, C., & Mitchum, G. (2010). Estimating mean sea level change from the TOPEX and Jason altimeter missions. *Marine Geodesy*, *33*(S1), 435–446.

Newman, M., Alexander, M. A., Ault, T. R., Cobb, K. M., Deser, C., Di Lorenzo, E., … Nakamura, H. (2016). The Pacific Decadal Oscillation, revisited. *Journal of Climate*, *29*, 4399–4427.

Nieves, V., Willis, J. K., & Patzert, W. C. (2015). Recent hiatus caused by decadal shift in Indo-Pacific heating. *Science*, *349*(6247), 532–535.

Nurhati, I. S., Cobb, K. M., & Di Lorenzo, E. (2011). Decadal-scale SST and salinity variations in the central tropical Pacific: Signatures of natural and anthropogenic climate change. *Journal of Climate*, *24*(13), 3294–3308.

Paillard, D., Labeyrie, L., & Yiou, P. (1996). Macintosh program performs time-series analysis. *Eos Transactions AGU*, *77*(39), 379–379.

Phillips, H. E., Wijffels, S. E., & Feng, M. (2005). Interannual variability in the freshwater content of the Indonesian-Australian Basin. *Geophysical Research Letters*, *32*, L03603. https://doi.org/10.1029/2004GL021755

Qu, T., Du, Y., McCreary, J. P. Jr., Meyers, G., & Yamagata, T. (2008). Buffering effect and its related ocean dynamics in the Indonesian throughflow region*. *Journal of Physical Oceanography*, *38*(2), 503–516.

Rayner, N., Parker, D. E., Horton, E., Folland, C., Alexander, L., Rowell, D., … Kaplan, A. (2003). Global analyses of sea surface temperature, sea ice, and night marine air temperature since the late nineteenth century. *Journal of Geophysical Research*, *108*, 4407. https://doi.org/10.1029/2002JD002670

Ren, L., Linsley, B. K., Wellington, G. M., Schrag, D. P., & Hoegh-Guldberg, O. (2002). Deconvolving the δ18O seawater component from subseasonal coral δ18O and Sr/Ca at Rarotonga in the southwestern subtropical Pacific for the period 1726 to 1997. *Geochimica et Cosmochimica Acta*, *67*(9), 1609–1621.

Schrag, D. P. (1999). Rapid analysis of high-precision Sr/Ca ratios in corals and other marine carbonates. *Paleoceanography*, *14*(2), 97–102.

Schulz, M., & Mudelsee, M. (2002). REDFIT: Estimating red-noise spectra directly from unevenly spaced paleoclimatic time series. *Computers & Geosciences*, *28*(3), 421–426.

Smith, T. M., Reynolds, R. W., Peterson, T. C., & Lawrimore, J. (2008). Improvements to NOAA's historical merged land-ocean surface temperature analysis (1880–2006). *Journal of Climate*, *21*(10), 2283–2296.

Speich, S., Blanke, B., & Cai, W. (2007). Atlantic meridional overturning circulation and the Southern Hemisphere supergyre. *Geophysical Research Letters*, *34*, L23614. https://doi.org/10.1029/2007GL031583

Sprintall, J., & Révelard, A. (2014). The Indonesian throughflow response to Indo-Pacific climate variability. *Journal of Geophysical Research: Oceans*, *119*, 1161–1175. https://doi.org/10.1002/2013JC009533

Thompson, D. M., Cole, J. E., Shen, G. T., Tudhope, A. W., & Meehl, G. A. (2015). Early twentieth-century warming linked to tropical Pacific wind strength. *Nature Geoscience*, *8*(2), 117–121.

Tierney, J. E., Abram, N. J., Anchukaitis, K. J., Evans, M. N., Giry, C., Kilbourne, K. H., … Zinke, J. (2015). Tropical sea surface temperatures for the past four centuries reconstructed from coral archives. *Paleoceanography*, *30*, 226–252. https://doi.org/10.1002/2014PA002717

Tillinger, D., & Gordon, A. (2010). Transport weighted temperature and internal energy transport of the Indonesian throughflow. *Dynamics of Atmospheres and Oceans*, *50*(2), 224–232.

Tillinger, D., & Gordon, A. L. (2009). Fifty years of the Indonesian throughflow*. *Journal of Climate*, *22*(23), 6342–6355.

Trenberth, K. E. (2015). Has there been a hiatus? *Science*, *349*(6249), 691–692.

Trenberth, K. E., & Fasullo, J. T. (2013). An apparent hiatus in global warming? *Earth's Future*, *1*(1), 19–32.

van Oldenborgh, G. J., & Burgers, G. (2005). Searching for decadal variations in ENSO precipitation teleconnections. *Geophysical Research Letters*, *32*, L15701. https://doi.org/10.1029/2005GL023110

van Sebille, E., Sprintall, J., Schwarzkopf, F. U., Sen Gupta, A., Santoso, A., England, M. H., … Böning, C. W. (2014). Pacific-to-Indian Ocean connectivity: Tasman leakage, Indonesian throughflow, and the role of ENSO. *Journal of Geophysical Research: Oceans*, *119*, 1365–1382. https://doi.org/10.1002/2013JC009525

Wainwright, L., Meyers, G., Wijffels, S., & Pigot, L. (2008). Change in the Indonesian throughflow with the climatic shift of 1976/77. *Geophysical Research Letters*, *35*, L03604. https://doi.org/10.1029/2007GL031911

Woodruff, S. D., Worley, S. J., Lubker, S. J., Ji, Z., Eric Freeman, J., Berry, D. I., … Smith, S. R. (2011). ICOADS release 2.5: Extensions and enhancements to the surface marine meteorological archive. *International Journal of Climatology*, *31*(7), 951–967.

Wyrtki, K. (1987). Indonesian through flow and the associated pressure gradient. *Journal of Geophysical Research*, *92*(C12), 12,941–12,946.

Zinke, J., Hoell, A., Lough, J., Feng, M., Kuret, A., Clarke, H., … McCulloch, M. (2015). Coral record of southeast Indian Ocean marine heatwaves with intensified Western Pacific temperature gradient. *Nature Communications*, *6*, 8562.